CLM-P785

CLM-P785

UKAEA

Preprint

COMPARISON OF THEORY WITH EXPERIMENT IN THE CONTEXT OF RECENT TOKAMAK ELECTRON CYCLOTRON CURRENT DRIVE RESULTS FROM WT-2

R. O. DENDY
M. O'BRIEN
M. COX
D. F. H. START

CULHAM LABORATORY
Abingdon, Oxfordshire
1986

CLM-P785

COMPARISON OF THEORY WITH EXPERIMENT IN THE CONTEXT OF RECENT TOKAMAK ELECTRON CYCLOTRON CURRENT DRIVE RESULTS FROM WT-2

R.O. Dendy, M. O'Brien, M. Cox, and D.F.H. Start

Culham Laboratory, Abingdon, Oxfordshire OX14 3DB, U.K.

(Euratom/UKAEA Fusion Association)

Abstract

A simple analytical model of the non-Maxwellian electron velocity distribution, whose parameters are constrained by the observed plasma current and soft X-ray emission spectrum, is used in conjunction with a fully three-dimensional ray-tracing code to calculate the absorption of radiation in the electron cyclotron range of frequencies by WT-2 discharges. This gives a quantitative theoretical description of the way in which a drifting population of energetic electrons appears to dominate WT-2 current drive experiments. Calculation of the proportion of source power absorbed by the plasma helps to determine the efficiency factor of the current drive mechanism in this context. The strong dependence of current drive on extraordinary mode launch direction is given quantitative theoretical support.

(Submitted for publication in Nuclear Fusion)

August 1986

I. INTRODUCTION

It has recently been reported that electron cyclotron current drive has been observed on the WT-2 tokamak.[1] This tokamak has major and minor radii $R_o = 40$ cm and $a = 9$ cm respectively, and toroidal field $B_T \leq 15$ kG. Under certain circumstances, a plasma current $I_p \simeq 3$ kA generated in the Ohmic phase could be maintained for 10 ms in the RF phase using ≤ 70 kW of output from a gyrotron of frequency $\omega/2\pi = 35.6$ GHz. The bulk electron temperature was 70 eV, the central electron density $n_e(0) \simeq 10^{12}$ cm^{-3}, and it was suggested that the current was supported by an electron beam containing a fraction μ of order one per cent of the total number of electrons. We refer to the original report[1] for further details. It is of interest to confront theory with the experimental results. In particular, we have numerical codes which calculate the absorption of electron cyclotron waves by non-Maxwellian electron velocity distributions in tokamaks, and also the soft X-ray emission spectram for arbitrary electron velocity distributions. We shall investigate the extent to which these codes and the associated theory can give a quantitative appraisal of the experimental results.

Three basic heating methods were employed in the experiment, all of which involve a launch position on the low-field side of the fundamental electron cyclotron resonance: (1) Extraordinary mode, propagating at 48° to B_T; (2) Ordinary mode, propagating perpendicular to B_T; (3) Extra-ordinary mode, propagating at -48° to B_T. In all three cases, the loop voltage V_L in the RF phase was substantially below that in the Ohmic phase. Only in case (1), however, was V_L found to pass below zero. In

cases (2) and (3), V_L did not reach zero, so that the current was not actually sustained in the absence of or against the loop voltage. Furthermore, the change $V_L(OH) - V_L(RF)$ is the same in cases (2) and (3) within the limits of experimental accuracy. This independence in cases (2) and (3) of the initial launch angle and polarisation suggests that the dominant wave-particle interactions occur only after a randomising process has destroyed the initial launch characteristics. Case (1) is thus distinct from cases (2) and (3) in two important respects. Firstly, V_L passes below zero in case (1) so that current drive is more effective in this case, and must be occurring in addition to any enhancement in conductivity due to generalised heating. Secondly, initial launch angle and polarisation do not appear to matter greatly in the less effective cases (2) and (3), which suggests that these characteristics do matter in the more effective case (1).

In this paper, we address the question: why is case (1) singled out in this way? We note that for the configurations considered, the low-density extraordinary mode cutoff lies between the launch position of the wave and its fundamental electron cyclotron resonance. It is therefore difficult to see how the wave in case (1) can resonate with the bulk thermal plasma electrons without invoking multiple reflections that would destroy the initial launch characteristics, which as we have seen do appear to matter. There are thus grounds for supposing that the wave damps on any electrons in the current-carrying superthermal population that lie between the launch position and the low-density X-mode cutoff. Such electrons could pass into cyclotron resonance with the incident wave due to the Doppler effect.

In the next Section, we construct a model for the electron velocity distribution which is consistent as far as possible with the experimental constraints. These constraints are provided by the value of the plasma current and the observed soft X-ray spectrum. In Section III, we outline the basis of our ray-tracing code. This code gives an accurate quantitative description in toroidal geometry of the absorption of waves in the electron cyclotron range of frequencies by a wide range of non-Maxwellian velocity distributions. In Section IV, we check the validity in the present context of the nonrelativistic approximation employed in Section III. In Section V, the experimentally consistent distribution function derived in Section II is used in the ray-tracing code of Section III, and the results are discussed in relation to the WT-2 electron cyclotron current drive results. In particular, we calculate the proportion of the applied power which is absorbed by the electrons on the first pass. This enables us to calculate the efficiency of the basic electron cyclotron current drive mechanism for this tokamak in this configuration. We present our conclusions in Section VI.

II. THE ELECTRON VELOCITY DISTRIBUTION FUNCTION

We shall fit the electron velocity distribution function $f(v_\perp, v_\parallel)$ to the following model:

$$f(v_\perp, v_\parallel) = \frac{(1-\mu)\pi^{-3/2}}{v_B^3} e^{-v_\perp^2/v_B^2} e^{-v_\parallel^2/v_B^2}$$

$$+ \frac{\mu\pi^{-3/2}}{v_B^2 v_T} e^{-v_\perp^2/v_B^2} e^{-(v_\parallel - v_o)^2/v_T^2} \qquad (1)$$

Here $v_\perp$ and $v_\parallel$ denote respectively the components of electron velocity perpendicular and parallel to the magnetic field. The three parameters (μ, v_o, v_T) characterise the superthermal deviation of the distribution from a bulk Maxwellian; in general, $\mu << 1$. By suitable choice of (μ, v_o, v_T), Eq.(1) can represent both monotonically decreasing superthermal tails and beam-like bump-on-tail distributions. Analytical[2,3] and numerical ray-tracing[3,4] studies have been carried out on the absorption of extraordinary mode electron cyclotron waves by distributions which have the form of Eq.(1).

Constraints on the numerical values of the set (μ, v_o, v_T) in representing the WT-2 discharge are provided by the experimentally determined plasma current and soft X-ray spectrum. We assume a parabolic electron density profile $n_e(r) = n_e(0)(1 - r^2/a^2)$, where r denotes distance from the magnetic axis and the values of $n_e(0)$ and a have been given in Section I. Integrating this profile over the plasma volume, and $v_\parallel$ times Eq.(1) over velocity space, we obtain the plasma current

$$I_p = \mu\left(\frac{v_o}{v_B}\right)\left(\frac{n_e(0)}{10^{12}\text{cm}^{-3}}\right)\left(\frac{T_B}{10\text{eV}}\right)^{1/2}\left(\frac{a}{10\text{cm}}\right)^2 4.8\ \text{kA} \qquad (2)$$

Here T_B denotes the bulk electron temperature associated with the bulk thermal velocity v_B, and the effect of electron trapping arising from the toroidal magnetic field geometry has been neglected. The experimentally determined parameters thus give rise to the constraint

$$\mu(v_o/v_B) \simeq 0.3 \qquad (3)$$

A code has been developed[5] to calculate the soft X-ray emission spectrum[6] from an arbitrary electron velocity distribution. Subject to Eq.(3) and to the experimental requirement that $\mu \lesssim$ a few times 0.01, we have varied the parameters v_o and v_T so as to reproduce from the code a good fit to the observed soft X-ray emission spectrum. We find that the best fit to these two key experimental constraints is given by

$$(\mu,\ v_o,\ v_T) = (0.03,\ 11\ v_B,\ 11\ v_B) \qquad (4)$$

for the representation of Eq.(1); see Fig.1, which can be compared with Fig.2(a) of Ref.1. We emphasise that these results are specific to our choice of tail model, and thus non-unique. Our primary aim here is to give a quantitative appraisal of the role of absorption by superthermal electrons in the WT-2 electron cyclotron current drive experiments. The precise form of the tail distribution in WT-2 may be continually evolving with time. At any instant it will be determined by a large number of effects, integrated back over time to the beginning of the discharge: inductive and RF electron acceleration, collisions, pitch-angle scattering, magnetic trapping, finite confinement time, and collective instabilities. Although research continues on this complex nonlinear problem, there is no general solution. Consequently we, like other

authors,[2-4,7] have relied on a relatively simple analytical model for the tail at a given instant, given in our case by Eqs.(1) and (4). This model does not correspond in detail to the tail formation, but is consistent at a more macroscopic level with the experimental constraints provided by the plasma current and the soft X-ray emission spectrum.

III. RAY-TRACING MODELLING OF WAVE ABSORPTION IN WT-2

The principles of tracing rays which are solutions of the localised dispersion relation in an inhomogeneous medium are well-known, and we refer elsewhere[8-10] for details. The Culham ray-tracing code[11] has recently been amended[3] to include the effects of absorption by non-Maxwellian velocity distributions represented by Eq.(1). The details of the underlying analysis are given in Ref.3. Here, we give only the warm-plasma dispersion relation for waves in the electron cyclotron range of frequencies which provides the basis for our modelling of absorption in the WT-2 discharge.

We define local plasma parameters $X = (\omega_p/\omega)^2$ and $Y = \Omega_e/\omega$, and note that absorption arises from the zeros of

$$\zeta = \frac{1 - Y}{N_\parallel v_B/c} \quad , \qquad \eta = \frac{1 - N_\parallel v_o/c - Y}{N_\parallel v_T/c} \tag{5}$$

In dealing with these resonances, we shall employ the nonrelativistic approximation; its applicability in our context will be discussed in detail in Section IV. The resulting complex dispersion relation takes the form $D^C + D^W = 0$, where D^C is the standard cold-plasma dispersion

relation and D^W contains additional warm-plasma terms from the bulk and tail contributions to Eq.(1). The imaginary part N_i of the refractive index, which describes wave absorption, is given to good approximation by[12]

$$N_i = \frac{-\,\mathrm{Im}\, D^W}{\frac{N_\parallel}{N}\frac{\partial D^C}{\partial N_\parallel} + \frac{N_\perp}{N}\frac{\partial D^C}{\partial N_\perp}} \tag{6}$$

Here $N_\perp = N\sin\theta$ and $N_\parallel = N\cos\theta$ denote the components of the refractive index N perpendicular and parallel to the local direction of the magnetic field. In Eq.(6),

$$\mathrm{Im}\, D^W = \frac{\pi^{1/2}|N_\parallel| v_B/c}{|Z(\zeta)|^2}(1+Y)\left\{\Gamma_1 e^{-\zeta^2} + \frac{2\mu\Gamma_2}{N_\parallel v_T/c}\left[F(\zeta)e^{-\eta^2} - F(\eta)e^{-\zeta^2}\right]\right\} \tag{7}$$

Here Z denotes the plasma dispersion function,[13] $F(x) = e^{-x^2}\int_0^x e^{t^2}dt$ is the Dawson integral, and

$$\Gamma_1 = D_1 + D_2 \quad , \qquad \Gamma_2 = \frac{X}{2}D_o + (1-Y)D_2 \tag{8}$$

$$D_o = \sin^2\theta\, N^4 - \left[2\left(1 - \frac{X}{1+Y}\right)\sin^2\theta + (1-X)(1+\cos^2\theta)\right]N^2 + 2(1-X)\left(1 - \frac{X}{1+Y}\right) \tag{9}$$

$$D_1 = \left[\left(1 - \frac{X}{2(1+Y)}\right)\sin^2\theta + (1-X)\cos^2\theta\right]N^4$$

$$- \left[\left(1-\frac{X}{2(1+Y)}\right)(1-X)(1+\cos^2\theta) + \left(1-\frac{X}{(1+Y)}\right)\sin^2\theta\right]N^2 + (1-X)\left(1-\frac{X}{(1+Y)}\right) \tag{10}$$

$$D_2 = \frac{X}{Y}\sin^2\theta\, N^2(N^2-1+\frac{X}{1+Y}) + \frac{1}{4}\frac{X^2}{Y^2}\frac{\sin^2\theta}{\cos^2\theta}\left[1+\cos^2\theta)N^2 - 2(1-\frac{X}{1+Y})\right]$$

$$+ \frac{1}{2}\frac{X(1-Y)}{Y^2}\frac{\sin^2\theta}{\cos^2\theta}\left[\cos^2\theta\, N^4-(1-\frac{X}{2(1+Y)})(1+\cos^2\theta)N^2 + (1-\frac{X}{1+Y})\right] \tag{11}$$

In Section V, we shall employ the tail parameters deduced in Section II in Eqs.(6)-(11), which have been implemented in the ray-tracing code. Before doing so, however, we shall examine the applicability in our context of the nonrelativistic approximation.

IV. NONRELATIVISTIC APPROXIMATION

The analysis in Section III was carried out in the nonrelativistic approximation. That is, the dependence of the electron cyclotron frequency on velocity through the relativistic variation of mass was neglected. The conditions for the validity of this approximation when the electron velocity distribution is non-Maxwellian remain a topic for research,[14,15] which is generally based on an examination of the original integral expressions for the dielectric tensor elements obtained by Shkarofsky.[16] Accordingly, we rely here on the conditions which apply to a Maxwellian plasma. For oblique propagation of the extraordinary mode, and absorption well away from the fundamental cyclotron resonance of the

bulk thermal electrons, the most restrictive condition for validity is[15]

$$N_{\parallel}^2 >> \left|(\omega - \Omega_e)/\Omega_e\right| \qquad (12)$$

The variation of Ω_e with distance R from the tokamak axis of symmetry is $\Omega_e \sim 1/R$, and for fundamental electron cyclotron resonance at the plasma centre, $\omega = \Omega_e(R_o)$. Then by Eq.(12), the nonrelativistic approximation remains valid for given $N_{\parallel}$ so long as the value of R where absorption occurs satisfies

$$\left|(R - R_o)/R_o\right| << N_{\parallel}^2 \qquad (13)$$

As stated previously, $R_o = 40$ cm and $a = 9$ cm for WT-2. Consider absorption at the outer edge, where Eq.(13) will be most difficult to satisfy; say $R = 48$ cm. Then Eq.(13) requires $N_{\parallel}^2 > 1/6$. The launch angle for the extraordinary mode in the experiments is $\pm 48°$ to B_T, in which case $N_{\parallel}^2 = 1/2$ and Eq.(13) is satisfied reasonably well. For absorption close to the centre of the plasma, Eq.(13) is satisfied by a greater margin. We conclude that the nonrelativistic approximation used in Section III is valid in our context.

V. RESULTS OF CALCULATIONS

We now present the results of the analytical and numerical approach to the WT-2 electron cyclotron heating and current drive results[1] that we have developed in the preceding Sections. The parameters of Eq.(4), which refer to a distribution whose form is given by Eq.(1), are substituted into Eqs.(5)-(11) as implemented in the ray-tracing code. A poloidal

projection of eight extraordinary mode rays launched from the outside of the tokamak in a cone of semiangle 6° at 48° to the magnetic field direction is shown in Fig.2. Each cross represents a 5% decrement in the power in a ray. The vertical dashed line represents the fundamental electron cyclotron resonance, and the curves are respectively the extraordinary mode upper hybrid resonance and low-density cutoff. It is clear from Fig.2 that substantial absorption takes place in the plasma between the radiation source and the cutoff. We find that the fraction α of the incident power absorbed by the electrons is $\alpha = 93\%$. This determines the efficiency η_{EC} of the electron cyclotron current drive mechanism for this configuration,

$$\eta_{EC} = I_p / \alpha P_{EC} \tag{14}$$

where $P_{EC} \simeq 70$ kW is the gyrotron power. Since $I_p = 3$ kA, our determination of α yields $\eta_{EC} = 4.6 \times 10^{-2}$ AW^{-1}. This figure is more than an order of magnitude smaller than that typically obtained in lower hybrid current drive experiments.[1,17,18] Scaling the PLT[17] and Alcator-C[18] lower hybrid current drive efficiency to the WT-2 discharge, we obtain an efficiency of order thirty times η_{EC}. We note that this low value for η_{EC} occurs even in a configuration where, as in the case of lower hybrid current drive, wave damping is concentrated exclusively on the most energetic electrons whose collisionality is correspondingly lowest. In drawing this comparison, it is essential to calculate the value of α in Eq.(14), as we have done. The experimentally observed electron cyclotron current drive efficiency falls well below the value expected from fundamental theory,[19] and from our Fokker-Planck code.[5] Using simple assumptions, a theoretical current drive efficiency of

approxomately 5 AW^{-1} is indicated. This large discrepancy points to the importance of the factors that we have not been able to include in the Fokker-Planck calculation. These include collective instabilities of the superthermal tail, and information about the energy and particle confinement times, together with the initial state of the electron velocity distribution at the onset of the RF phase. a full treatment of this essentially nonlinear, intrinsically unstable, driven system, taking account of the initial conditions set by the Ohmic phase, is at present beyond the scope of the theoretical techniques at our disposal. However, our calculation of the energy deposition profiles is less sensitive to these factors, and we now consider these quantitative results in greater detail.

Smooth spatial power deposition profiles have been obtained by using a large number of rays. For Fig.3, one hundred and eight were traced. Here the power deposited per unit area on a toroidal surface at a distance $\bar{r}$ from the magnetic axis is plotted as a function of r. Power deposition is concentrated in the hollow toroidal plasma volume located between 3.5 cm and 5.5 cm from the magnetic axis, where Eq.(13) is well satisfied. The consequences for stability of the associated localisation of the plasma current invite further investigation. In Fig.4, the power deposition is shown as a function of parallel electron velocity. The role of the low-density plasma cutoff in preventing absorption for $v_{\parallel} < 9v_B$ can be clearly seen. Absorption is strongest in the range $10v_B < v_{\parallel} < 16v_B$, which by Eqs.(1) and (4) is the region of velocity space where the density of tail electrons is greatest.

Finally, we find that for launch angles counter to the direction of the drift velocity v_o, no cyclotron resonance with plasma electrons is

possible on the first pass. The rays are refracted back out of the plasma onto the vacuum chamber wall. It is probable that subsequent multiple reflections and mode conversions will eventually lead to some absorption. However, a launch angle in the same sense as v_o is clearly singled out as favourable for current drive by its very high first pass absorption on the drifting electron population.

VI. CONCLUSIONS

In making our appraisal of the WT-2 electron cyclotron current drive results,[1] we have employed a number of analytical and numerical methods. These include: a simple analytical model for the non-Maxwellian electron velocity distribution, whose parameters are constrained by the observed plasma current and by the requirement that the associated soft X-ray emission spectrum, obtained numerically, coincide with that observed; and a fully three-dimensional ray-tracing code which calculates the absorption of radiation in the electron cyclotron range of frequencies by the non-Maxwellian electron velocity distribution in the toroidal geometry of WT-2.

This approach has given a quantitative description of the way in which a drifting population of energetic electrons appears to dominate absorption in WT-2 current drive experiments. Because of the Doppler shift, such electrons can enter into cyclotron resonance with the radiation if they are physically present in the plasma between the launch position and the extraordinary mode cutoff, which shields the fundamental resonance of the bulk electrons. For a launch angle at 48° to the magnetic field direction in the same sense as the electron drift, we

calculate that 93% of the incident extraordinary mode power is absorbed by the energetic electrons in the first pass. This figure enables us to determine the efficiency of the electron cyclotron current drive mechanism in this context. The efficiency is an order of magnitude less than in lower hybrid current drive, despite the fact that in both cases wave damping is concentrated on the most energetic, least collisional electrons. For an extraordinary mode launch angle of -48°, there is no first pass absorption. Although multiple reflections and mode conversions will eventually lead to some absorption in this case, our calculations indicate how the positive launch angle is singled out for effective current drive.

REFERENCES

[1] A. Ando, K. Ogura, H. Tanaka, M. Iida, S. Ide, K. Oho, S. Ozaki, M. Nakamura, T. Cho, T. Maekawa, Y. Terumichi, and S. Tanaka, Phys. Rev. Lett. 56, 2180 (1986).

[2] I. Fidone, G. Granata, and R.L. Meyer, Plasma Phys. 22, 261 (1980).

[3] A. Montes and R.O. Dendy, Culham Laboratory Preprint CLM-P755, accepted for publication in Phys. Fluids.

[4] A. Montes and R.O. Dendy, Proc. Course and Workshop on Applications of RF Waves to Tokamak Plasmas, Varenna (Monotypia Franchi, Perugia, 1985), Vol.II, p.770.

[5] M. O'Brien, M. Cox, and D.F.H. Start, to be published in Nuclear Fusion.

[6] J.E. Rice, K. Molvig, H.I. Helava, Phys. Rev. A 25, 1645 (1982).

[7] L. Muschietti, K. Appert, and J. Vaclavik, Phys. Fluids 24, 151 (1981).

[8] S. Weinberg, Phys. Rev. 126, 1899 (1962).

[9] I.B. Bernstein, Phys. Fluids 18, 320 (1975).

[10] M. Brambilla and A. Cardinali, Plasma Phys. 24, 1187 (1982).

[11] P.J. Fielding, private communication.

[12] A.I. Akhiezer, I.A. Akhiezer, R.V. Polovin, A.G. Sitenko, and K.N. Stepanov, Plasma Electrodynamics (Pergamon, Oxford, 1975), Vol.I.

[13] B.D. Fried and S.D. Conte, The Plasma Dispersion Function (Academic, New York, 1961).

[14] I. Fidone, G. Granata, and R.L. Meyer, Phys. Fluids, 25, 2249 (1982).

[15] M. Bornatici, R. Cano, O. De Barbieri, and F. Engelmann, Nucl. Fusion 23, 1153 (1983).

[16] I.P. Shkarofsky, Phys. Fluids 9, 561 (1966).

[17] R. Motley, S. Bernabei, T.K. Chu, P. Efthimion, W. Hooke, F. Jobes, J. Stevens, E. Valeo, and S. von Goeler, Proc. IAEA Technical Committee Meeting on Non-Inductive Current Drive in Tokamaks (Culham Laboratory, U.K., 1983), Vol.II, p.299.

[18] M. Porkolab, J.J. Schuss, B. Lloyd, Y. Takase, S. Texter, P. Bonoli, C. Fiore, R. Gandy, D. Gwinn, B. Lipschultz, E. Marmar, D. Pappas, R. Parker, and P. Pribyl, Phys. Rev. Lett. 53, 450 (1984).

[19] N.J. Fisch and A.H. Boozer, Phys. Rev. Lett. 45, 720 (1980).

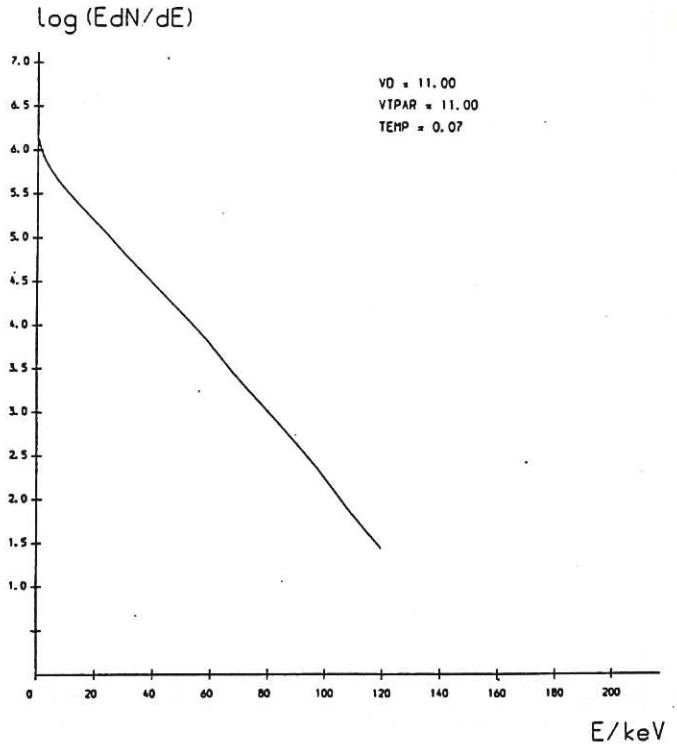

Fig. 1 Soft X-ray emission spectrum (arbitrary units) computed for the parameters of Eq. (4) in Eq. (1).

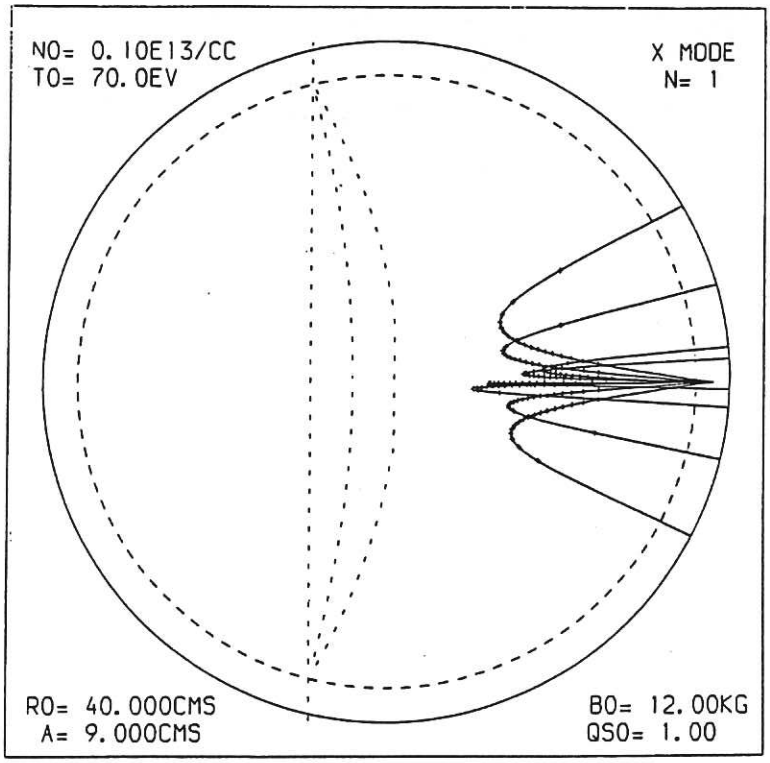

Fig. 2 Poloidal projection of extraordinary mode rays for low-field side launch at 48° to the magnetic field direction. Central electron density $10^{12}\,cm^{-3}$, temperature 70 eV, and toroidal magnetic field 12 kG. The superthermal tail is described by Eqs. (1) and (4). Each cross on a ray marks a five percent decrement in power. The dashed lines are, from left, the fundamental electron cyclotron resonance and the extraordinary mode upper hybrid resonance and low-density cutoff.

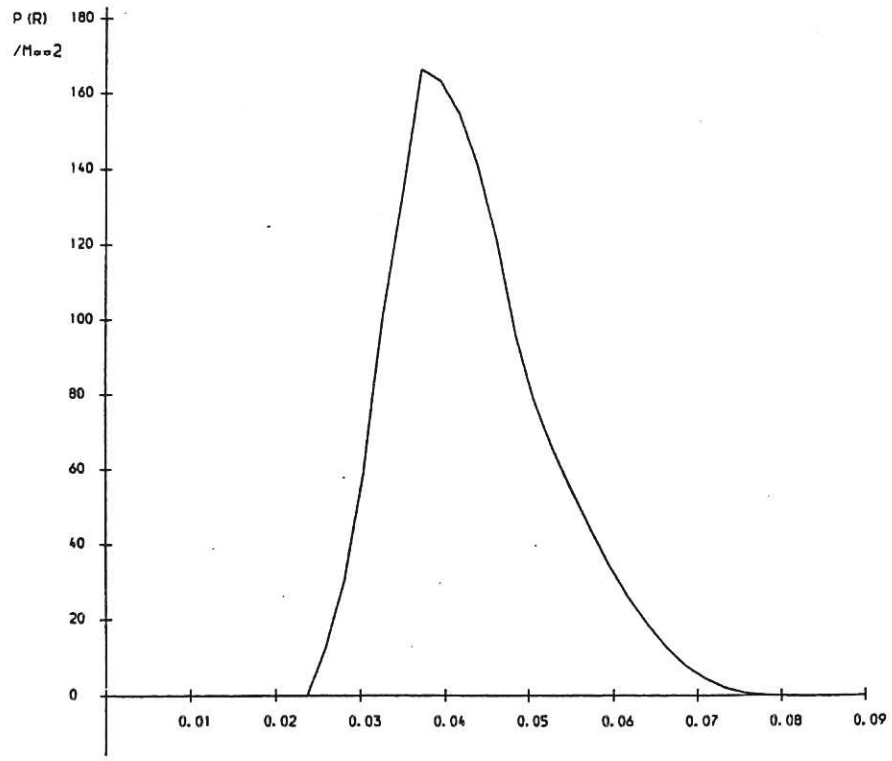

Fig. 3 Spatial power deposition profile: power deposited per unit area on a toroidal surface at a distance r from the magnetic axis as a function of r.

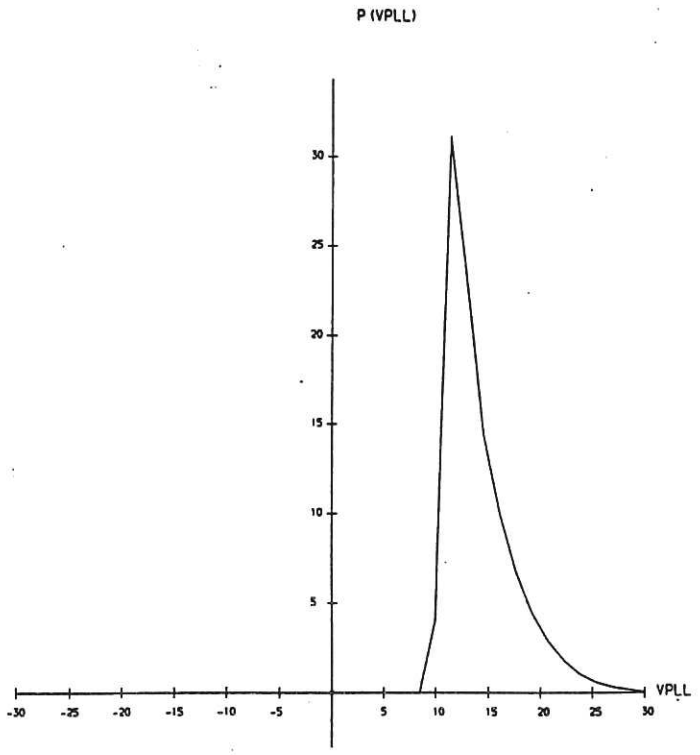

Fig. 4 Velocity space power deposition profile: power deposited per unit interval of $v_{\|}/v_B$ as a function of $v_{\|}/v_B$.

CLM-P785